Multiple Approaches for Ultrasonic Cavitation Monitoring of Oxygen-Loaded Nanodroplets

Simone Galati, Adriano Troia

Abstract—**Ultrasound(US) is widely used in medical field for a variety diagnostic techniques but, in recent years, it has also been creating great interest for therapeutic aims. Regarding drug delivery, the use of US as an activation source provides better spatial delivery confinement and limits the undesired side effects. However, at present there is no complete characterization at a fundamental level of the different signals produced by sono-activated nanocarriers. Therefore, the aim of this study is to obtain a metrological characterization of the cavitation phenomena induced by US through three parallel investigation approaches. US was focused into a channel of a customized phantom in which a solution with oxygen-loaded nanodroplets (OLNDs) was led to flow and the cavitation activity was monitored. Both quantitative and qualitative real-time analysis were performed giving information about the dynamics of bubble formation, oscillation and final implosion with respect to the working acoustic pressure and the type of nanodroplets, compared with pure water. From this analysis a possible interpretation of the observed results is proposed.**

Keywords—**Cavitation, Drug Delivery, Nanodroplets, Ultrasound.**

I. INTRODUCTION

EXPLOITATION of the cavitation phenomena generated by ultrasound-activated nanocarriers is gaining a significant role in both diagnostic and therapeutic medical applications in recent decades. In particular, a set of well-developed imaging techniques has been proposed showing several benefits in different branches of medicine [1]. In US imaging techniques, images are generated by measuring the propagation of high-frequency sound waves travelling into tissues and by exploiting specific compressible carriers (bubbles) as contrast agents: an oscillation in the acoustic field is generated producing nonlinear responses of these bubbles that can be distinguished from surrounding tissues, amplifying the ultrasound signal. Since this method is reported to have several advantages (high sensitivity, portability, low cost and good safety profile), it is now one of the most used in the medical imaging [2].

In addition to their diagnostic capability and thanks to their structure, carriers can be loaded with molecules, drug and gene as well as functionalized with ligands, thereby giving the possibility to reach specific targets of the human body [3]. These methods can be thus expanded to promising therapeutic techniques, such as gene and drug delivery. In more detail, the encapsulated drug is dependent on the type of sonocarrier exploited: when using nanoparticles, for example, drug molecules or reactive oxygen species (ROS) can be stored and delivered, while pharmaceutical or gas molecules can be loaded when using nanobubbles or nanodroplets.

Recently, research has shown an increased interest in the development of new oxygen carriers for treating tissue hypoxia diseases due to the fact that the current hyperoxygenation techniques have several drawbacks. New perfluorocarbon-based nanobubbles formulations have been proposed as they provide promising properties. First of all they are soluble molecules useful for stabilizing gas; moreover they are highly stable and bioinert [4]. Furthermore, changing their physical and chemical properties it is possible to set both the boiling temperature at which perfluorocarbons are able to vaporize into bubbles and also the diffusion velocity of the inner gas. This is indeed inversely proportional to the dimension of the carriers: the lower their radius, the higher the differential gas pressure and the faster the gas diffusion, according to the Laplace law for spherical surfaces [5]. Another advantage regards the fact that the interaction between the bubbles and the acoustic field leads to a local modulation of permeability of both the cell membranes and microvasculature, enhancing the release of drug in the desired area. All of this has led to the development of new oxygen-loaded nanobubbles (OLNBs) cored with perfluoropentane (PFP) and shelled with chitosan which show efficient, stable and biocompatible oxygen delivery [6]. These OLNBs have provided the basis for the synthesis of another new platform of nanocarriers: oxygen-loaded nanodroplets(OLNDs) with a core structure of liquid decafluorpentane (DFP) at body temperature [7], that have been shown to have higher efficiency in gas release with respect to the nanobubbles, while confirming all the other favorable properties.

There are many principles behind the activation of nanodroplets and the consecutive release of gas; these are due to the interaction between the acoustic field and the liquid solution. Firstly, US induces bubble formation after acoustic droplet vaporization (ADV), a phase shift of the droplets into their vapor form (bubbles) [8]. In general in a liquid solution, bubble formation is caused by two main mechanisms: the first regards the gas present in the solution, the second involves the presence of impurities that transport gas acting as cavitation nuclei. After bubbles are generated, the sinusoidal acoustic pressure variation that the ultrasonic field generates leads to their consecutive oscillation until the cavitation phenomenon [9]. The presence of a periodic pressure variation induced by the acoustic field allows the bubbles to expand during the rarefraction phase (the negative peak of the sinusoidal cycle)

S. Galati is with the Department of Electronics and Telecommunications, Polytechnic University of Turin and with the Department of Metrology of Advanced Materials and Life Science, Istituto Nazionale di Ricerca Metrologica, Turin, IT (e-mail: simone.galati@polito.it).

A. Troia is with the Department of Metrology of Advanced Materials and Life Science, Istituto Nazionale di Ricerca Metrologica, Turin, IT (e-mail:a.troia@inrim.it).

and to compress during the positive cycle. This alternation generally goes on for a few acoustic cycles leading the bubbles to reach a resonance size: when this happens, they may undergo either a violent collapse (transient or inertial cavitation) or a stable linear oscillation near the resonant size (stable cavitation). The cavitation phenomenon is regulated by the properties of the liquid (vapor pressure and viscosity [10], [11]) as well as the type of sonosensitive carriers that are involved (nanoparticles, nanobubbles, nanodroplets) and, depending on the type of cavitation, several effects can be observed [12]. During oscillations, stable cavitation is characterized by microstreaming and Bjerkness secondary forces: the first produces a vortex with shear forces that can be strong enough to break particles or to permeabilize cells; the second forces, due to their attractive and repulsive nature, can attract particles close to the bubbles and release their content because of the shear forces. In bubble collapse (inertial cavitation), a formation of shock waves with high pressure is induced and, owing to translational motion of the bubbles, a jet stream of liquid that can pass through the bubbles and hit the objects in the surrounding zones may occur. This event has been demonstrated to lead to a number of uncontrollable side bioeffects that may be dangerous for the surrounding cells and structures and, for this reason, it is important to avoid it. To this aim, the working acoustic pressure range has to be defined in order to limit the inertial cavitation activity.

Although several works explore these techniques, they mostly focus on in-vitro/vivo studies without a complete characterization of the basic phenomenon. For this reason, this study is focused on the optimization of a setup to induce the cavitation of specific kind of droplets in order to observe their response through a complete characterization of the different signals (acoustic, ecographic and optical) generated by the US-nanocarriers interaction.

II. METHODOLOGY

A. OLNDs Preparation and Characterization

Two different types of liquid nanodroplets were prepared, using PVA and chitosan as coatings. In order to obtain a liquid formulation of OLNDs [7], by means of Ultra-Turrax SG215 homogenizer, at first, 1.5 ml DFP with 0.5 ml PVP and 1.8 ml Epikuron 200 were homogenized in 30 ml of water for 2 minutes at 24000 rpm. Then, the solution was saturated with O_2 for more 2 minutes. Lastly, 1.5 ml of chitosan or PVA solution was added drop-wise during the final homogenization of the mixture at 13000 rpm for 2 more minutes.
The final OLNDs were then characterized in their sizes and distribution through the Dynamic Light Scattering (DLS) technique (Delsa Nano C Particle Analyzer, Beckman Coulter) and in their shape by means of an optical microscope. Fig. 1 provides the dimension distribution of a sample of chitosan coated OLNDs measured by DLS, while in Fig. 2 the PVA shelled droplets observed at optical microscope are shown. From the DLS results the average diameter of the PVA droplets was about ~ 400nm, while chitosan OLNDs were larger, with an average diameter of ~ 600nm; the microscope analysis
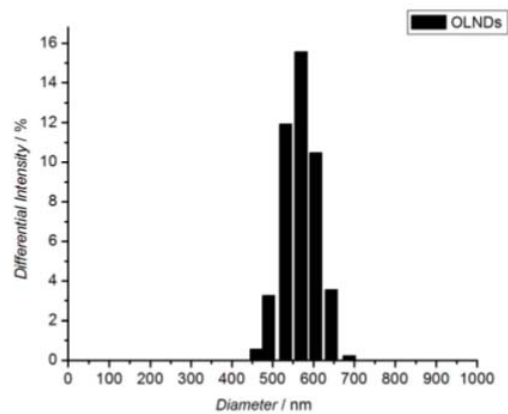

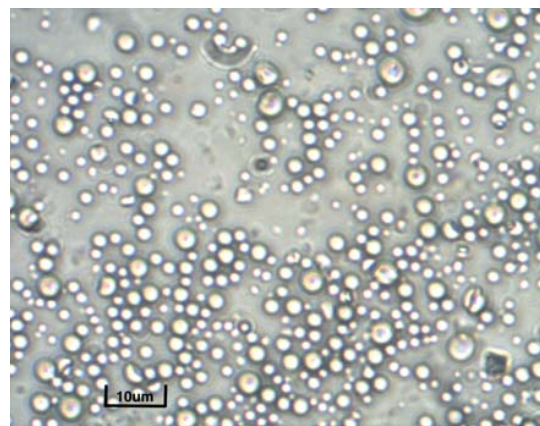Fig. 1 Chitosan-coated OLNDs size distribution from DLS analysis

Fig. 2 PVA-coated OLNDs at the optical microscope with a magnification of 40X

showed a spherical shape for both types of OLNDs. Only larger bubbles population was visible in this case.

B. Phantom Preparation

The solutions with the particles under test were led to flow into a channel in a customized phantom made of materials able to mimic the acoustic properties of human soft tissues. Two different phantom recipes were tested in this work with the same geometry and dimensions but with different physical properties. To this aim, a plastic cylindrical mould was used, with two opposite holes on the external surface in which a small tube (diameter ~ 3.5mm) for the channel shaping was inserted. The first phantom used was a transparent silicon-based polymer (Bluesil RTV $141A/B$). Once the components were mixed, the solution was dipped into the mould and put in an oven at $38°$C for 24 hours in order to initiate the vulcanization process.
The second phantom was a soft gel based on Gellan Gum (GG) polysaccharide. Briefly, a 1.5% in weight solution of GG was heated up to $70°$C until the solution was clear. Then it was poured into the mould and left cooling. In order to increase the
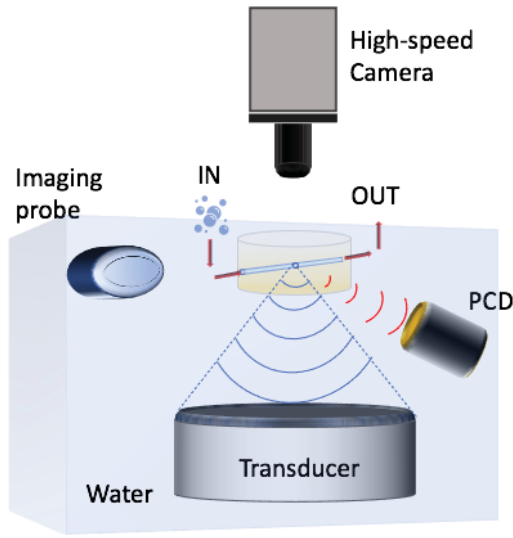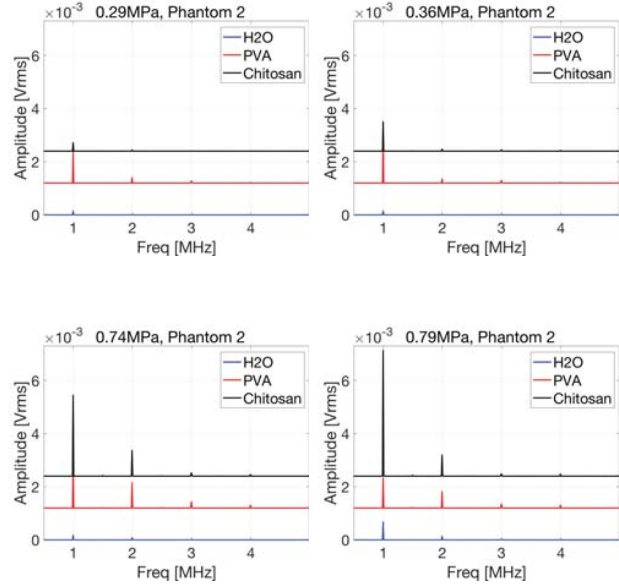
Fig. 3 Scheme of the experimental setup

Fig. 4 FTT spectra of chitosan- and PVA-coated OLNDs compared with respect to pure water at different acoustic pressures, 0.29 MPa (Fig. 4A), 0.36MPa (Fig. 4B), 0.74MPa (Fig. 4C) and 0.79MPa (Fig. 4D). Each plot shows the overlap of the spectra for the three solutions with the ones related to PVA and chitosan that have been shifted in the y direction in order to have better visibility and comparison

mechanical and attenuation properties of the gel, it was dipped for 24 hours in a 0.4 Molar solution of zinc acetate, exploiting the crosslinking mechanism promoted by divalent ions. Further details about preparation and the acoustic properties can be found here [13].

C. Experimental Setup for Cavitation Activity Detection

A scheme of the experimental setup is presented in Fig. 3. The US excitation was given by a focused US (Sonic Concepts H-101) transducer working at a fundamental frequency $f = 1MHz$ driven by A&R amplifier (model 800A3A) connected with function generator (Agilent 33250A). By means of a hydrophone coupled to an oscilloscope (InfiniiVision 2000 X DSO-X 2022A, Agilent Technologies) the Peak Rarefractional Pressures (PRPs) were measured and stored on a Labview-provided PC resulting in a working acoustic pressure range between $0.2 - 0.8$ MPa for the experiments reported there. The solution was injected into the channel using a manual flow controller (Cole Parmer Masterflex Peristaltic Pump) and the acoustic cavitation activity was monitored by acquisition of the broadband acoustic signal in the range of 500kHz - 5MHz, by means of a focused Passive Cavitation Detector (PCD) (Ultrasonic Transducer PA1101, Precision Acoustics) connected to a spectrum analyzer (Keysight N9320b, Agilent). The resulting FFT spectra were characterized by the presence of peaks at specific frequencies revealing the activity of stable cavitation, due to the forced bubbles oscillations. Recorded data were stored and plotted with Matlab highlighting the presence of ultra-harmonics and harmonics with respect to the fundamental driving frequency. In Fig. 4 acoustic spectra at different acoustic pressures for the two OLNDs solutions compared with the pure water are shown. In order to have a quantitative indicator of the bubble collapse (inertial cavitation), the spectra were processed to perform the cavitation noise spectrum analysis. Basing on the

assumption that the continuous components of the spectrum between harmonics and ultra-harmonics (the so-called "white noise") are originated from the shock waves during the inertial cavitation activity, the analysis were performed through the evaluation of cavitation noise power indicator (CNP) [14] as follows. Starting from the stored data, they were manipulated through Matlab in order to pass from linear to logarithmic scale following the formula:

$$I_{dB} = 20 \log_{10}(I_{mV}/I_0) \qquad (1)$$

where the I_0 value is the minimum acquired by the spectrum analyzer for each spectrum. At this point, the spectra were filtered of all the harmonics and ultra-harmonics components in order to emphasize the contribution of the white noise and, at the end, the filtered logarithmic data were integrated over frequency according to

$$CNP = \int I_{dB}(f)df \approx \sum I_{dB}(f)\Delta f \qquad (2)$$

where $I_{dB}(f)$ is the spectrum amplitude in logarithmic scale and f the frequency.

Although the obtained values were not related to a physical power, they were linked to the white noise power generated by the bubble collapse activity and so it could be used as a measure of the inertial cavitation activity.

D. Ultrasound Imaging

Ultrasonic imaging investigations were carried out using an ultrasonic research scanner (Ultrasonix SonixTouch) connected to a linear probe (SA4-/24, Ultrasonix) operating at

$10 MHz$, positioned in front of the phantom. B-mode imaging was used to align the channel of the phantom with respect to the focus of the transducer and to collect the OLNDs real time responses during ultrasound irradiation. The recorded videos were then processed with Matlab in order to monitor the average intensity of the bright spots inside a specific region of interest (ROI) during the ultrasound irradiation. This method allowed to carry out a qualitative measure of the bubbles formation and oscillation to be correlated with the evaluation of cavitation activity.

E. Optical Imaging

The third sensor that was added to the setup is a high-speed camera (CamRecords 5000, Optronis) put directly on the channel in order to get an optical observation of the phenomena. In order to ensure the visibility to be localized onto the channel, a light source (MultiLED G8 power supply and MultiLED QT white, GS Vitec) was placed on the top of the phantom, opportunely tilted for optimizing the amount of light focused on zone of interest. Although the used camera was able to record with a maximum rate of 5000 fps, the measures were performed at 3000 fps in order to maximize visibility, magnification and resolution as much as possible. No ADV dynamics could be appreciated at this recording frame speed but it was sufficient for observing the dynamic interaction of the bubbles with the acoustic field and to determine the different behavior for the two tested sono-carriers.

III. RESULTS AND DISCUSSION

The experiments demonstrate the expected response of the droplets to the US activation. The FFT spectra analysis (Fig. 4) shows the presence of peaks at different frequencies for the OLNDs with respect to the pure water. This confirms that the ultrasound response was enhanced by the presence of the droplets in the solution. In particular, the spectra were characterized by various discrete frequency components around nf/m, where f is the fundamental working frequency ($f_0 = 1 MHz$), while m, n are integers. These components are the harmonics and ultra-harmonics and are due to the non-linear characteristic of the stable cavitation, so to the forced pulsations generated by the interaction between the bubbles and the ultrasonic field [15]. Furthermore, increasing the acoustic pressure, a different behavior between the PVA- and chitosan-coated droplets was observed. Using PVA, well detectable peaks related to stable cavitation appeared even at low acoustic pressures. As pressure increased, moreover, the amplitude of the peaks remained constant but higher ultra-harmonics related to the presence of non-linear oscillations appeared. Regarding the chitosan-coated droplets on the other hand, only the fundamental peak increased at low pressures, while ultra-harmonics started to be present only up to $0.74 MPa$.

Analyzing the filtered broadband spectra, the cavitation noise power was evaluated for all the solutions at different pressures. Fig. 5 shows the numerical results of the CNP parameter for all the three different solutions as function
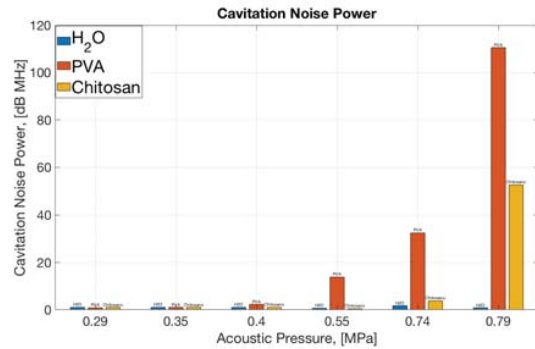

Fig. 5 Cavitation Noise Power comparison between pure water, PVA-coated nanodroplets and chitosan-coated nanodroplets at different acoustic pressures

of the increasing acoustic pressures. The parameter related to pure water did not show a significant rise, confirming that no cavitation activity, neither stable nor inertial, was present. On the other hand regarding the droplets response, it could be noticed how PVA-OLNDs entered the inertial cavitation phase at lower acoustic pressure values with respect to chitosan-OLNDs, which showed a remarkable amount of inertial activity only for the highest value of acoustic pressure ($P_a = 0.79 MPa$). These data were in good correlation with the qualitative ones discussed with the FFT spectra. In particular, they allowed to understand which were the upper pressure limits to avoid the activation of inertial cavitation phenomena for the two different sono-carriers in order to prevent the unwanted side bioeffects due to the violent bubbles collapse.

The results obtained with ultrasonic imaging probe require further considerations. Fig. 6 shows the recorded images for all the three tested solutions at two limit values of acoustic pressure ($P_{a_{low}} = 0.39 MPa$ - $P_{a_{high}} = 0.79 MPa$), while Fig. 7 summarizes the average intensities of the light spots recorded into the selected ROI over about 13 seconds of acoustic field exposure. As expected, there was no substantial difference increasing the acoustic pressure when water flowed (Fig. 6 A-B). On the contrary analyzing PVA-OLNDs, the different amount of bubbles formation and oscillation was well visible into the selected region from $P_a = 0.39$ MPa to $P_a = 0.79$ MPa (Fig. 6 C-D). A similar variation on the area was observed using also the chitosan-coated droplets (Fig. 6 E-F). However their higher intensity evaluated into the ROI (Fig. 7) suggests that, because of the more rigid shell structure due to chitosan, the population which went under the ADV mechanism was lower for these OLNDs that tent to remain trapped into acoustic antinodes giving a more intense signal on the imaging probe. On the other hand, PVA-based ones suddenly disappeared once ADV transition was completed. This behavior was also confirmed by the presence of more intense light spot usually related to the presence of air into the solution, giving evidence again of the inertial cavitation activity that was more prominent with the PVA-coated droplets.

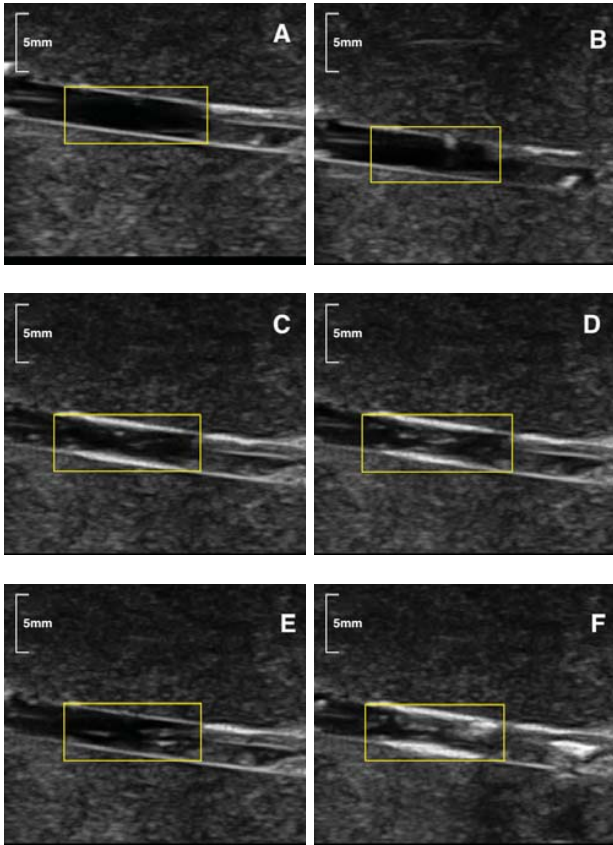Finally, Figs. 8 and 9 report the high-speed frames for

Fig. 6 Frames of the recorded videos with the US imaging probe a two different acoustic pressures (0.39MPa for the first column and 0.79MPa for the second one) respectively for pure water (A-B), PVA-coated nanodroplets (B-C) and chitosan-coated nanodroplets (E-F)
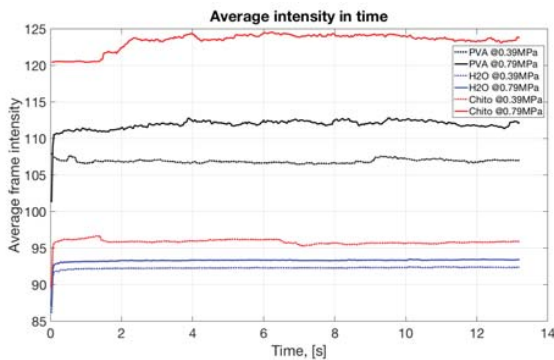

Fig. 7 Comparison of the average intensity of the light spots measured into the ROI shown in Fig. 6 at $P_a = 0.39$MPa and $P_a = 0.79$MPa for each solution
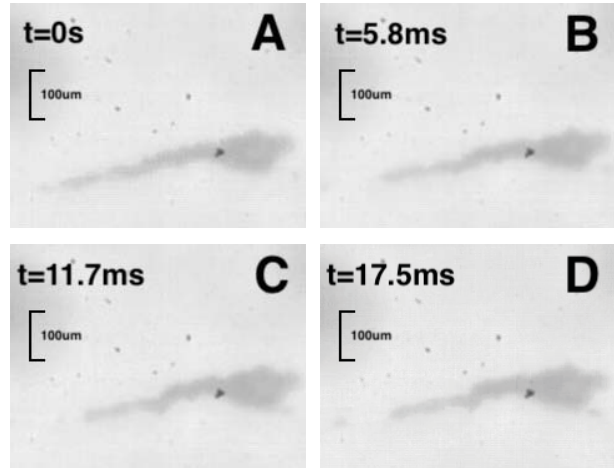

Fig. 8 Frames recorded with the high-speed camera with a frame rate of 3000 fps at different time of the PVA-coated OLNDs at acoustic pressure $P_a = 74$MPa
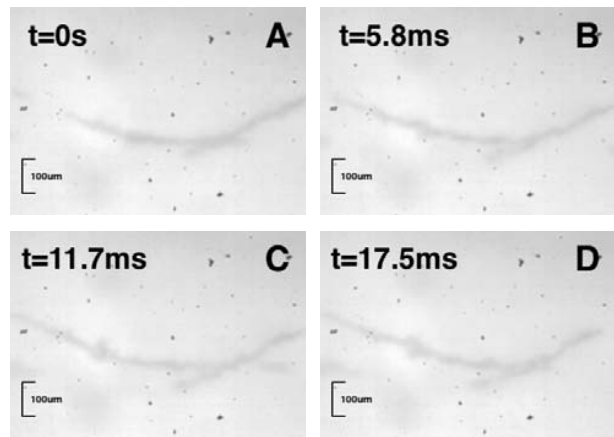

Fig. 9 Frames recorded with the high-speed camera with a frame rate of 3000 fps at different time of the chitosan-coated OLNDs at acoustic pressure $P_a = 74$MPa

both types of droplets flowing inside the channel. In order to appreciate the dynamics of droplets the recording time started after 5s of ultrasonic exposure. From the recorded videos, droplets oscillations could be observed. Depending in particular on their dimension, the bigger the droplets the lower was their response to the US field. Furthermore it can be noticed how the bubbles generated by PVA-based droplets were led to agglomerate towards a fixed position along the acoustic field lines forming clusters, while in chitosan-coated they merged in lines apparently without forming any bigger cluster. This could be seen as another confirmation of the two different behaviors for these droplets, as evidenced by previous results.

IV. CONCLUSION

In the present study, multiple approaches for the monitoring of the ultrasound-induced cavitation phenomena in in-vitro setup using different drug delivery carriers have been presented. In particular, the setup was optimized in order to exploit three different investigation methods for the signals emitted by the interaction between ultrasound and nanocarriers. The ultrasonic field was focused on the solution flowing in a customized phantom with a channel and a PCD, a high-speed camera and an ultrasonic imaging probe were placed around it in order to acquire respectively the acoustic, optical and ecographic responses. Two different kinds of oxygen-loaded nanodroplets were tested, one PVA-coated and

the other chitosan-coated, and all the measures were performed using pure water as reference solution.

All three approaches produced coherent results, making it possible to characterize the same phenomenon from different points of view. Both PVA- and chitosan-coated OLNDs showed stable cavitation activity starting from low acoustic pressures. Starting from this, the working range of the acoustic pressures could be defined for both solutions in order to avoid inertial cavitation thanks to different intensity in harmonics and ultra-harmonics together with differences on the cavitation noise analysis. From these analysis it emerged that for PVA-based OLNDs the working pressure range was lower. This phenomenon was also confirmed by the imaging investigation with the ultrasonic probe: some intensive light spots, typical of the presence of air, in this case due to ADV phenomenon and subsequent bubbles collapse, were detected more when using PVA. Finally, the high-speed camera videos showed a more intensive agglomeration and merging of the PVA-coated OLNDs due to an intensification of the attractive forces which characterize the cavitation phenomena and lead to the consequent bubbles collapse (inertial cavitation).

These results indicated that the characterization of the ultrasound activated drug delivery of perfluorocarbon-based nanodroplets requires a multiple approach in order to better investigate the dynamics of different nanocarriers exposed in flowing channel to simulate real conditions. Future studies could improve the optical setup of the camera in order to increase magnification and resolution thus obtaining more information about the acoustic droplet vaporization transition and further correlations between the acoustic signals emitted during stable bubbles oscillations and the cavitation activity.

References

[1] E.P. Stride and C.C. Coussions, *Cavitation and contrast: the use of bubbles in ultrasound imaging and therapy*, Proceedings of the Institution of Mechanical Engineers, Part H: Journal of Engineering in Medicine, 2010, 224, 171-191.

[2] A. Zlitni and S.S. Gambhir, *Molecular imaging agents for ultrasound*, Current Opinion in Chemical Biology, 2018, 45, 113-120.

[3] K.H. Martin and P.A. Dayton, *Current status and prospects for microbubbles in ultrasound theranostics*, WIREs Nanomed Nanobiotechnol 2013, 5, 329345.

[4] E.G. Schutt and D.H. Klein and R.M. Mattrey and J.G. Riess, *Injectable microbubbles as contrast agents for diagnostic ultrasound imaging: the key role of perfluorochemicals.*, Angew Chem Int Ed Engl. 2003, 42(28), 3218-35.

[5] A. Sanfeld and K. Sefiane and D. Benielli and A. Steinchen, *Does capillarity influence chemical reaction in drops and bubbles? A thermodynamic approach*, Advances in Colloid and Interface Science, 2000, 86(3), 153-193.

[6] A. Bisazza and P. Giustetto and A. Rolfo and I. Caniggia and S. Balbis and C. Guiot and R. Cavalli, *Microbubble-mediated oxygen delivery to hypoxic tissues as a new therapeutic device.*, Annu Int Conf IEEE Eng Med Biol Soc. 2008, 2008,2067-70.

[7] C. Magnetto and M. Prato and A. Khadjavi and I. Fenoglio and J. Jose and G. R. Giulino and F. Cavallo and E. Quaglino and E. Benintende and G. Varetto and A. Troia and R. Cavalli and C. Guidot, *Ultrasound-activated decafluoropentane-cored and chitosan-shelled nanodroplets for oxygen delivery to hypoxic cutaneous tissues*, RSC Adv, 2014, 4, 38433-38441.

[8] O.D. Kripfgans and J.B. Fowlkes and D.L. Miller and O.P. Eldevik and P.L. Carson, *Acoustic droplet vaporization for therapeutic and diagnostic applications*, Ultrasound Med Biol, 2000, 26(7),1177-89.

[9] P. Poritsky, *The collaps or growth of a spherical bubble or cavity in a viscous fluid*, Proceedings of the 1st US National Congress in Applied Mathematics (ASME), 1952.

[10] J. Jiao and Y. He and K. Yasui and S.E. Kentish and M. Ashokkumar and R. Manasseh and J. Lee, *Influence of acoustic pressure and bubble sizes on the coalescence of two contacting bubbles in an acoustic field*, Ultrasonics Sonochemistry, 2015, 22, 70-77.

[11] S. Popinet and S. Zaleski, *Bubble collapse near a solid boundary: a numerical study of the influence of viscosity*, Journal of Fluid Mechanics, 2002, 137-163.

[12] T. Boissenot and A. Bordat and E. Fattal and N.Tsapis, *Ultrasound-triggered drug delivery for cancer treatment using drug delivery systems: From theoretical considerations to practical applications*, Journal of Controlled Release, 2016, 241, 144-163.

[13] A. Troia and R. Cuccaro and A. Schiavi, *Independent tuning of acoustic and mechanical properties of phantoms for biomedical applications of ultrasound*, Biomed. Phys. Eng. Express, 2017, 3.

[14] J. Frohly and S Labouret and C Bruneel and I Looten-Baquet and R. Torguet, *Ultrasonic Cavitation Monitoring by Acoustic Noise Power Measurement.*, The Journal of the Acoustical Society of America. 2000, 108, 2012-20.

[15] J. Wu and S. Zhou and X. Li, *Acoustic emission monitoring for ultrasonic cavitaiton based dispersion process*, Journal of Manufacturing Science adn Engineering, 2013, 135.

Simone Galati Simone Galati is a second year Ph.D student in Metrology at Politecnico di Torino in collaboration with INRIM. His doctoral research investigates the acoustic cavitation phenomena for drug delivery systems. He graduated at Politecnico di Torino in Physical engineering and Nanotechnologies for ICT's with a master thesis project on Hollow MEMS microfabrication carried out at Denmarks Tekniske Universite.

Adriano Troia Adriano Troia is a Ph.D. in Science of Materials and a resercher at INRIM form 2012. He 's author of several peer review papers in the field of cavitation, tissue mimicking materials and nanodroplets for drug delivery. He has been leading European projects in field of metrology and author of international patent on nanodroplets fabrication.